Thick-Target $O^{16}(d,n)F^{17}$ Yield Curves*

R. M. Bahnsen,† W. R. Wylie,‡ and H. W. Lefevre
University of Oregon, Eugene, Oregon 97403
(Received 1 October 1969; revised manuscript received 2 April 1970)

A thick-target method has been used to measure absolute differential cross sections for the reactions $O^{16}(d,n)F^{17}$ and $O^{16}(d,n)F^{17*}$(0.500 MeV) from 2.0 to 4.2 MeV. Excitation functions were taken at 20° intervals from 0–160° in the lab system. Satisfactory fits to the angular distributions required Legendre polynomials of order 6 or higher. The c.m. Legendre coefficients A_0 and A_1 are presented as a function of lab deuteron energy for the ground-state data. The total cross sections for production of ground-state and first-excited-state neutrons are also given as a function of energy.

I. INTRODUCTION

Previous work at the University of Oregon has shown that it is possible to transform the continuous neutron spectrum produced by charged-particle bombardment of a thick target into a yield curve.[1,2] This method has been used to study the $O^{16}(d,n)F^{17}$ reaction at bombarding energies up to 4.2 MeV. Reactions induced by low-energy deuterons usually show evidence of both compound-nucleus (CN) and direct-reaction (DR) contributions. The angular distributions resemble stripping curves and are indicative of DR effects, while the yield curves generally show structure indicative of significant CN contributions. Thick-target methods[1,2] provide an efficient means of studying such reactions, since it is possible to map out the yield surface of the reaction in only a few days of accelerator running time. Oxygen is a frequent target contaminant, and an additional incentive to this work is that accurate cross-section data on the $O^{16}(d,n)F^{17}$ reaction may be of use in the analysis of data from other (d,n) reactions.

The $O^{16}(d,n)F^{17}$ reaction has been studied previously by several authors. In 1955, Marion, Brugger, and Bonner,[3] using "long counter" and "counter ratio" methods, measured the ground-state and first-excited-state thresholds as 1.830 and 2.393 MeV, establishing the energy of the F^{17} first excited state to be 0.499 ± 0.003 MeV. Their zero-degree yield curve taken with relatively low angular resolution showed evidence for 10 peaks in the 9.5–11.0-MeV excitation region of the F^{18} compound system. Only peaks below 2.393-MeV bombarding energy could be definitely assigned to structure in the yield of neutrons to the F^{17} ground state.

The positions of a number of peaks in the ground-state and ground plus first-excited-state neutron data agreed with the proton data of Van Patter *et al.*[4] on the mirror $O^{16}(d,p)O^{17}$ reaction. The (d,p) reaction was also studied by Stratton *et al.*,[5] who measured a number of angular distributions, and ground-state and first-excited-state yield curves at 53°, the experimentally determined position of the ground-state stripping peak. Analysis of the data led to an $l=2$ momentum transfer, in agreement with the measured $\frac{5}{2}$ spin and the shell-model's $1d_{5/2}$ picture of the O^{17} ground state.[6] The strong forward peaking of the first-excited-state proton group was taken to imply an $l=0$ transfer, in agreement with the shell-model's $2s_{1/2}$ prediction for this state.[6]

Yaramis has studied the $O^{16}(d,n)F^{17}$ reaction at 5.02 MeV.[7] Absolute ground-state and first-excited-state cross sections were measured using a gas recoil counter and CO_2 gas targets. Dimensionless reduced widths (θ's) were found to be 0.025 (0.0-MeV level) and 0.15 (0.500-MeV level). The analysis of the first-excited-state data was hampered by the fact that it is bound against proton decay by only 96 keV.

Dietzsch *et al.*[8] have studied deuteron-induced reactions on O^{16} from 2.0–3.5 MeV, and have measured absolute differential cross sections for the elastic scattering, the ground-state and first-excited-state neutrons and protons, and the ground-state α particles. The data were analyzed using the optical-model, Hauser-Feshbach theory, and the distorted-wave Born approximation. Spectroscopic factors were obtained from fitting energy-averaged experimental data.

II. METHOD AND EQUIPMENT

The thick-target method uses targets made of materials with low atomic number, which are thick compared with the range of the incident charged-particle beam in the target material, but thin compared with the mean free path of the product neutrons. A beam of charged particles incident on such a target loses energy mainly by ionizing the target material. Nuclear reactions removed approximately 1 deuteron in 10^4 from the

incident beam, so that nearly all of the beam particles undergo the complete stopping process. The beam deviates very little from 0° as it slows down in the target. (For deuterons slowing down from 4.2–2.0 MeV, calculations based on Fermi's formula give $\theta_{rms} < 3°$).[1]

Nuclear reactions are thus induced by a beam of particles having a continuum of energies, and the resulting neutron time-of-flight (T-O-F) spectrum is likewise continuous. If the first excited state of the residual nucleus is at a high enough excitation energy (≳0.5 MeV), it is possible to separate the ground-state portion of the data and transform it into a yield curve. In the case of the $O^{16}(d,n)F^{17}$ reaction, the Q values and the low-lying structure of F^{17} are such that it is possible to get both ground-state and first-excited-state yield curves.

Figure 1 shows some sample neutron data – the γ-ray peaks are off scale at 3.3 nsec/m. The high-energy edge at the right of the 2.8-MeV data corresponds to ground-state neutrons produced by O^{16}-$(d,n)F^{17}$ reactions at the surface of the target. Neutrons below this edge were produced by deuterons which slowed down in the target before reacting. The edge at $1/v = 110$ nsec/m is due to the onset of first-excited-state neutrons. Below this edge the data arise from both ground-state and first-excited-state neutrons. The 0.5-MeV-wide region between the two edges may be referred to as a window. Data in this region are due entirely to ground-state neutrons. As the bombarding energy is increased, the window moves to higher neutron energies. Ideally a complete ground-state neutron spectrum could be obtained from the window portions of a series of runs spaced 0.500 MeV apart. The bombarding energy was actually changed in 0.200-MeV steps to allow for the resolution width, which is inevitably folded into the kinematic edges.

The deuteron beam was obtained from the University of Oregon's 4-MeV Van de Graaff accelerator. This machine is equipped with a terminal pulser and klystron buncher built by ORTEC, Inc. A countdown circuit in the terminal eliminates the retrace and allows the pulse spacing to be varied by factors of 2 from 0.5 to 16 μsec. The machine can deliver 1.5-nsec, full width at half maximum (FWHM), pulses on target at time-average currents of 1–10 μA.

A 1-mm-thick (liquid) water sample was used as the target. The water was held in a cell separated from the vacuum system by a 1.12-μ nickel foil. The water was circulated to remove beam heat and bubbles caused by radiolysis. The cell was insulated from ground so that the target current could be integrated. Provision was also made to continuously monitor the target pulse on a sampling oscilloscope. The performance of the liquid-target system was checked by taking $C^{12}(d,n)N^{13}$ thick-target data from the (d,n) reaction on benzene. The spectra obtained at 0° agreed within statistics (2%) with the data from graphite targets after corrections were made for the molecular stopping cross section of benzene.

Neutrons were detected in a 6.3-cm-diam × 1.2-cm-thick Naton scintillator optically coupled to a XP-1040 phototube. Signals from the fourteenth dynode and the anode triggered a low-walk timing discriminator.[9] A linear signal was obtained from the tenth dynode. This signal was connected to an ORTEC time-pick-off (TPO) discriminator which determined the detector bias. Outputs from the TPO and the timing discriminator, suitably delayed, were fed into a coincidence circuit which provided start pulses for an ORTEC time-to-amplitude converter (TAC). The TAC channel width and linearity were measured using a method described by Hatcher.[10] Stop pulses for the TAC were obtained from a ferrite core, concentric with the beam axis, 35 cm from the target. The TAC was used on its 500-nsec full-scale range. The output of the TAC was digitized, stored online in a PDP-7 computer, and written on magnetic tape at the end of each run for off-line analysis.

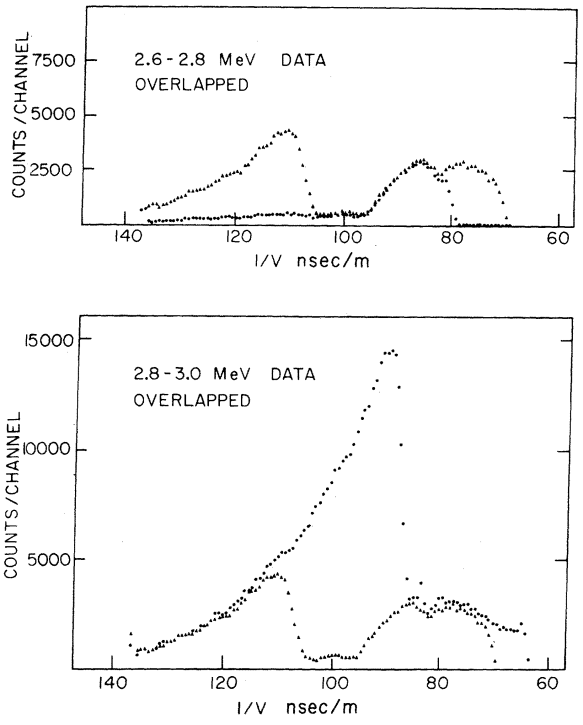

FIG. 1. Time-of-flight spectra showing the behavior of the kinematic edges. Only the ground-state edge appears in the 2.6-MeV data. Both ground- and first-excited-state edges appear in the higher-energy runs.

III. DATA ACQUISITION

Data were taken at 20° intervals from 0 to 160°. At each angle, runs were made consecutively from 2.6 to 4.2 MeV in 200-keV increments. Each run took about one-half hour during which 328 μC of charge, corrected for analyzer losses, were collected. Beam currents were limited to 0.5 μA to prolong foil life. The flight path was 3 m. Another series of runs was made with a 2-m flight path to measure the low-energy ground-state neutron yield with a better signal-to-background ratio. For these data, the machine energy was kept at 2.5 MeV and one run was taken at each angle from 0–160°.

Two different methods were used to correct for background. (1) For the 2.5-MeV run a 7.5-cm-diam by 54-cm-long brass bar was used to shadow the detector and obtain a background spectrum, which was subtracted from the foreground taken in another run. (2) For the 2.6–4.2-MeV runs, 1.02-m-diam by 44-cm-high cylindrical water tanks were centered above and below the target. The 10.5-cm gap between the tanks was filled with paraffin wedges. The wedge at the detector angle contained a collimator built according to the directions of Langsdorf.[11] This shield practically eliminated background and allowed data to be taken in one run. Tests indicated that both methods of background correction gave equivalent results. The water shield was used for the high-energy data (2.6–4.2 MeV), and the shadow bar was used for the 2.5-MeV runs purely as a matter of convenience.

IV. DATA REDUCTION

Data reduction was done off line on the PDP-7 computer. First, the window portions of the 2.6–4.2-MeV data were joined to produce a complete ground-state T-O-F spectrum. Once the complete ground-state T-O-F spectrum was obtained, the data below the first-excited-state kinematic edge of the 4.2-MeV run could be processed. The ground-state contribution was eliminated from the 4.2-MeV run by a subtraction procedure leaving a complete first-excited-state T-O-F spectrum.

Both T-O-F spectra were then transformed to yield curves using a histogram procedure in which a Fortran program was used to evaluate the following expression

$$\sigma_L(\theta)=\frac{N(t,\theta)dt}{N_d dE_d d\Omega\,\epsilon(E_n)}\,\frac{1}{n}\,\frac{dE_d}{dx},$$

where dt and $d\Omega$ are the spectrometer channel width and detector solid angle. The quantity N_d is the number of deuterons incident on the target, ϵ is the detector efficiency, and $(1/n)(dE_d/dx)$ is the molecular stopping cross section of the target.

The detector efficiency was expressed as a first-

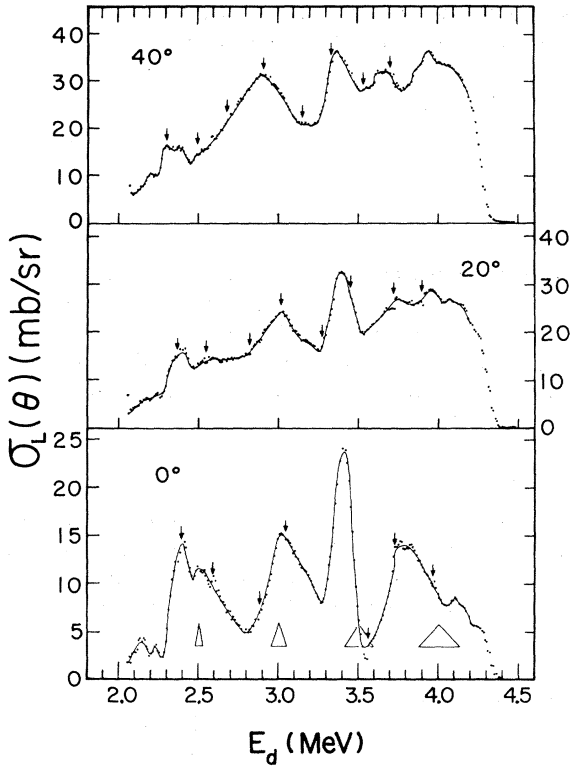

FIG. 2. Excitation functions for the $O^{16}(d,n)F^{17}$(ground-state) reaction. The arrows indicate the energies at which the data from successive runs were joined.

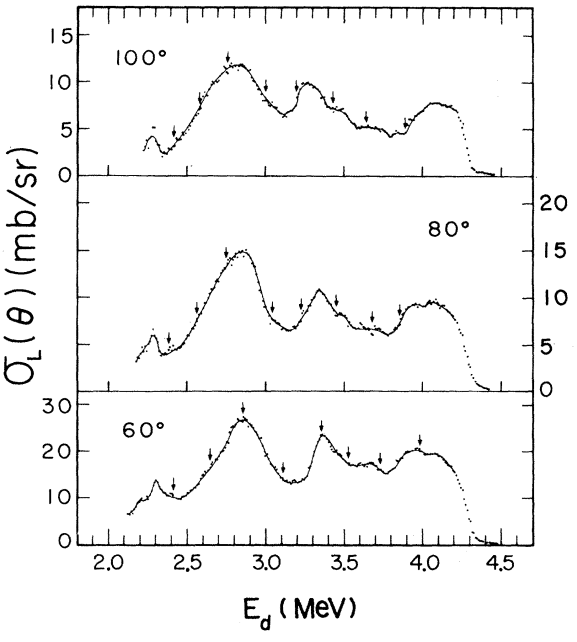

FIG. 3. Excitation functions for the $O^{16}(d,n)F^{17}$(ground-state) reaction.

order calculated efficiency multiplied by an experimentally determined correction function

$$\epsilon(E_n) = \epsilon_0(E_n) \cdot f(E_n).$$

The efficiency $\epsilon_0(E_n)$ was calculated from the expression

$$\epsilon_0(E_n) = (1 - e^{-n\sigma l})(1 - B/E_n),$$

where l is the scintillator length, n is the number of hydrogen atoms per cm^3, σ is the n-p total cross section, and B is the detector bias. The n-p total cross section was calculated using Gammel's semiempirical formula.[12] The constants in the correction function,

$$f(E_n) = 0.968 + (0.057)E_n,$$

were determined from thick-target studies of the $Li^7(p,n)Be^7$ and the $D(d,n)He^3$ reactions. Spectra have been presented elsewhere which give an indication of the accuracy of the calibration procedure.[13]

The molecular stopping cross sections were obtained by Bragg's rule, e.g., for water: $\epsilon_{H_2O} = 2\epsilon_H + \epsilon_O$. Published data indicate that Bragg's rule is applicable for deuterons above 300 keV,[14] so that its use in the 2–4-MeV range seems justified. The atomic cross section for hydrogen and

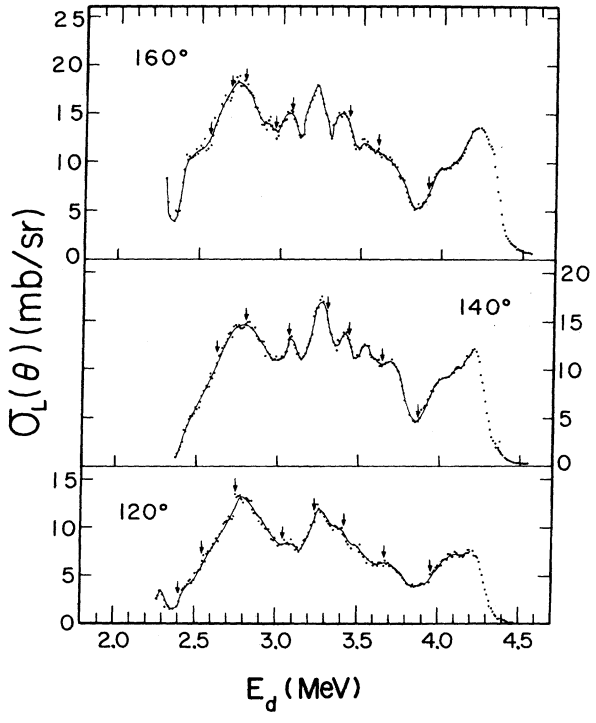

FIG. 4. Excitation functions for the $O^{16}(d,n)F^{17}$(ground-state) reaction.

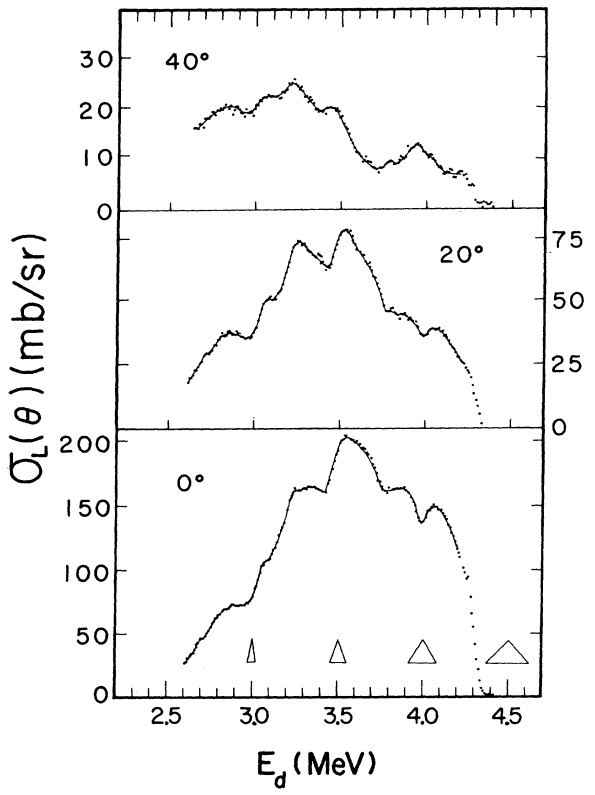

FIG. 5. Excitation functions for the $O^{16}(d,n)F^{17*}$(0.5-MeV state) reaction.

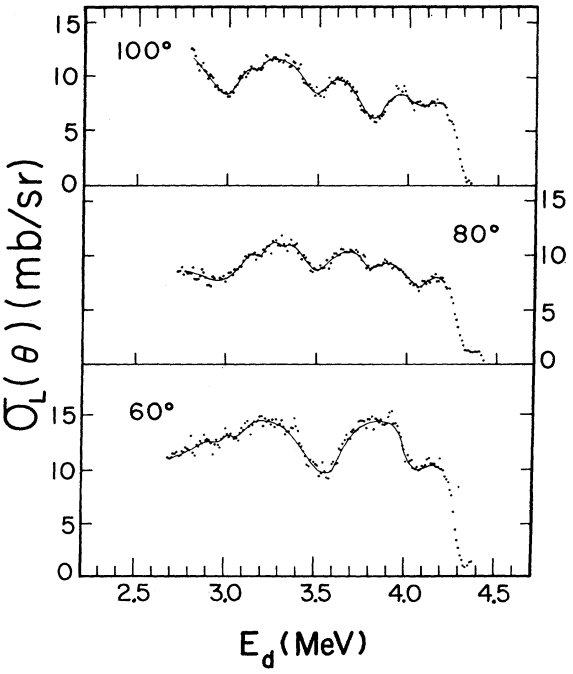

FIG. 6. Excitation functions for the $O^{16}(d,n)F^{17*}$ (0.5-MeV state) reaction.

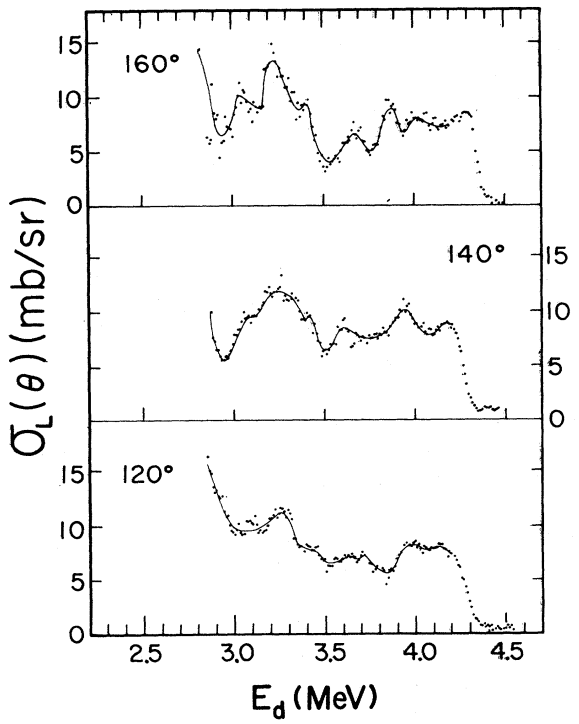

FIG. 7. Excitation functions for the $O^{16}(d,n)F^{17*}$ (0.5-MeV state) reaction.

oxygen were obtained from the Bethe-Block[15] formula using $I_H = 15.5$ and $I_O = 104.2$ eV. The calculated stopping cross sections agree with the 1.7% measurements of Reynolds *et al.*[14] in the range of energies covered by the experimental data, $E_d \leq 1.2$ MeV.

V. RESULTS AND DISCUSSION

The ground-state and first-excited-state differential cross sections are shown in Figs. 2-7. The arrows show the points at which the runs were matched and the resolution of the spectrometer is indicated by the FWHM of the triangles. The transformations were done at 10 keV per channel, which seems appropriate in view of the broadness of excitation-function structure at the lower energies, and the resolution width at the higher energies.

The statistical accuracy of the yield curves is determined by the number of counts per channel in the T-O-F spectrum. The error due to counting statistics is ≤2% for all data above 2.3-MeV bombarding energy. The transformation program was checked for systematic errors by successively applying the transformation program and its inverse to a set of data. Since the two programs employ quite different calculational methods, the fact that the T-O-F spectrum could be recovered provided reasonable assurance that the programs were executing properly.

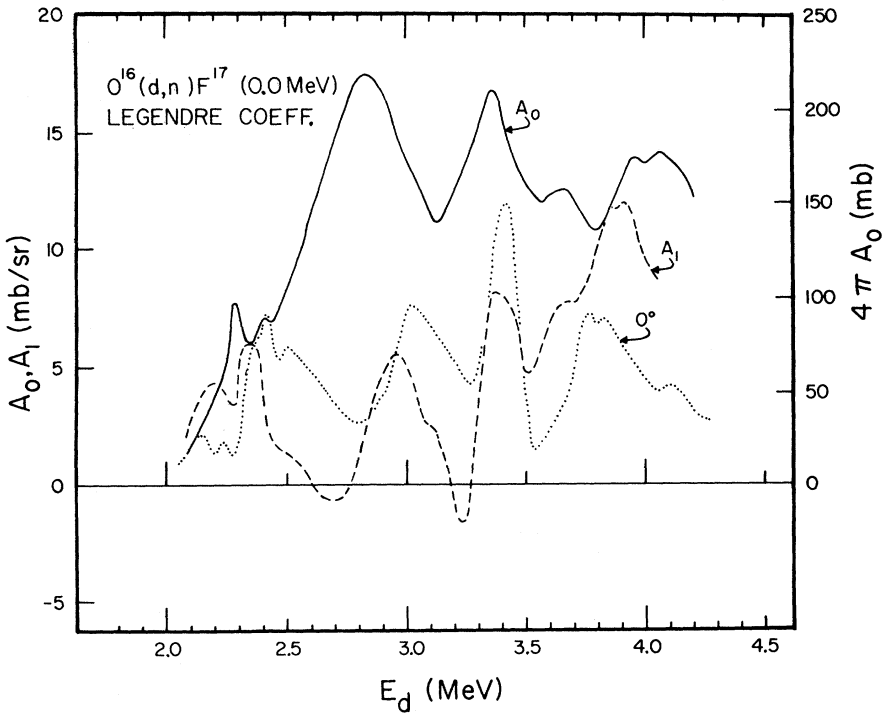

FIG. 8. Total cross section, A_0, A_1, and 0° differential cross section for the $O^{16}(d,n)F^{17}$(ground-state) reaction.

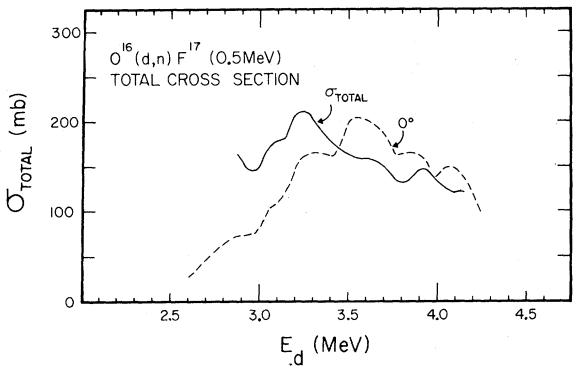

FIG. 9. Total cross section and 0° differential cross section for the $O^{16}(d,n)F^{17*}$ (0.5 MeV) reaction.

The detector angles could be set to ±0.5° and introduced a negligible error into the cross-section measurements. The error in the absolute calibration of the integrator was 5% and the error due to drift ≤1%. After the angular distribution was obtained the first run was repeated, and the two sets of data agreed within statistics.

The major uncertainties in the results are due to neutron scattering in the water target, and to the efficiency calibration of the detector. No corrections were made for scattering, but estimates of the outscattering indicate that it may be as high as 23% at 80 and 100° and ≤10% at all other angles. The detector efficiency is believed accurate to 10% for all data corresponding to neutron energies above 500 keV. The resulting uncertainties in the measured cross sections are 25% for the 80 and 100° data and 15% for all other angles. The cross sections agree with results of Dietzsch *et al.*[8] in the region of common bombarding energies.

There is a tendency for some of the peaks in the excitation function (e.g., the 0° ground-state peak at 3.2 MeV) to appear at lower energies at the backward angles. This is probably due to interference effects. If interference effects are important, peaks may be expected to show shifts with angle approximately equal to their widths, so that a peak in the yield curve at any one angle probably indicates that there are one or more F^{18} levels in the vicinity of the peak.

The ground-state data were fitted by Legendre polynomials using a least-squares procedure. Satisfactory fits to the data required polynomials up to order 6, inclusive. The coefficients A_0 and A_1 are shown in Fig. 8. The values for the total cross section obtained from $4\pi A_0$ are in good agreement with those obtained by integrating the experimental data over angle. The first-excited-state data were strongly peaked forward, and could not be satisfactorily fit by Legendre polynomials. For this reason the first-excited-state data were simply integrated over angle and the results are shown in Fig. 9.

Both the ground-state and first-excited-state total cross sections exhibit relatively little structure and show a rather strong resemblance to the 80 and 100° differential cross sections. They show relatively little resemblance to the forward and more highly structured backward-angle data, and very little resemblance to each other. These results are in qualitative harmony with the statistical picture of Dietzsch *et al.*[8] for F^{18} at these excitation energies.

VI. ACKNOWLEDGMENTS

The authors would like to thank C. A. Burke for his assistance during all phases of this work. Thanks are also due M. T. Lunnon and D. W. Kneff for their assistance in data collection, and to J. C. Overley who read the manuscript and provided helpful criticism.

---

*Work supported in part by the U. S. Atomic Energy Commission and by the University of Oregon Graduate School through a National Science Foundation "Centers of Excellence" grant.

†Present address: American Optical Company, Buffalo, New York.

‡Present address: Physik-Institüt der Universität Zürich, Zürich, Switzerland.

[1]W. R. Wylie, R. M. Bahnsen, and H. W. Lefevre, Nucl. Instr. Methods 79, 245 (1970).

[2]R. M. Bahnsen, W. R. Wylie, and H. W. Lefevre, Bull. Am. Phys. Soc. 12, 894 (1967).

[3]J. B. Marion, R. M. Brugger, and T. W. Bonner, Phys. Rev. 100, 46 (1955).

[4]D. M. Van Patter, B. E. Simmons, T. F. Stratton, and D. M. Zipoy, Phys. Rev. 96, 825 (1954).

[5]T. F. Stratton, J. M. Blair, K. F. Famularo, and R. V. Stuart, Phys. Rev. 98, 629 (1955).

[6]R. A. Laubenstein, M. J. W. Laubenstein, L. J. Koester, and R. C. Mobley, Phys. Rev. 84, 12 (1951).

[7]B. Yaramis, Phys. Rev. 124, 836 (1961).

[8]O. Dietzsch, R. A. Douglas, E. F. Pessona, V. G. Porto, E. W. Hamburger, T. Polga, and O. Sala, Nucl. Phys. 114, 330 (1968).

[9]D. L. Wieber and H. W. Lefevre, IEEE Trans. Nucl. Sci. 13 (No. 1), 406 (1966).

[10]C. Hatcher, EG&G Nanonotes 1, 2 (1964).

[11]A. Langsdorf, in *Fast Neutron Physics*, edited by J. B. Marion and J. L. Fowler (Interscience Publishers, Inc., New York, 1960), Vol. I, p. 721.

[12]J. L. Gammel, in *Fast Neutron Physics*, edited by J. B. Marion and J. L. Fowler (Interscience Publishers, Inc., New York, 1963), Vol. II, p. 2185.
[13]H. W. Lefevre and G. U. Din, Australian J. Phys. 22, 669 (1969).
[14]H. K. Reynolds, D. N. F. Dunbar, W. A. Wenzel, and W. Whaling, Phys. Rev. 92, 742 (1953).
[15]W. Whaling, in *Handbuch der Physik*, edited by S. Flügge (Springer-Verlag, Berlin, Germany, 1958), Vol. 34, p. 193.

PHYSICAL REVIEW C VOLUME 2, NUMBER 3 SEPTEMBER 1970

Λ-^{4}He Scattering at Low Energy

B. F. Gibson*
National Bureau of Standards, Washington, D.C. 20234

and

M. S. Weiss†
Lawrence Radiation Laboratory, University of California, Livermore, California 94550
(Received 16 March 1970)

The elastic scattering of the Λ particle by ^{4}He has been studied in the 0.1- to 10.0-MeV energy range. The calculation was performed using baryon-baryon interactions composed of central potentials previously employed in binding-energy calculations of $^5_\Lambda$He and a derivative spin-orbit Λ-^{4}He potential. Phase shifts, total cross sections, angular distributions, and polarizations were computed as functions of energy for $l=0$, 1, and 2. The results are sensitive to the potential parameters, implying that even simple measurements would yield interesting information.

I. INTRODUCTION

The importance of n-^{4}He and p-^{4}He scattering[1] to increasing our understanding of the nucleon-nucleon and the nucleon-nucleus systems leads one to suspect that a similar importance will eventually be attached to the scattering of Λ's from ^{4}He. At present there are no data available in the literature for such a reaction. We wish to examine the elastic scattering process with the view of indicating what might be expected experimentally. We hope that this type of study will help motivate such measurements. As will be discussed in Sec. V, even crude measurements would appear valuable.

As is the case in the n-^{4}He scattering system, we expect the Λ-^{4}He scattering to be particularly sensitive to any spin-orbit interaction. However, in the absence of a spin-orbit force and at energies below the breakup or excitation of ^{4}He, the scattering system is governed by the same potential that appears in the bound-state calculation of the hypernucleus $^5_\Lambda$He. Having recently examined the bound s-shell hypernuclei in the Hartree-Fock approximation,[2] we have available an effective s-wave Λ-N interaction which reproduces the experimental binding energy of $^5_\Lambda$He. (The potential is slightly weaker than would be deduced from the free Λ-N low-energy scattering parameters, an effect which is attributed to suppression[3] due to coupling to the Σ channel.) Moreover, our effective potential is almost of sufficient strength to bind the Λ in an $l=1$ orbital, where l is taken here with respect to the c.m. To the extent that the model is realistic, this limits the strength of any spin-orbit potential to values such that the lower-energy member of the $(j=\frac{1}{2},\ j=\frac{3}{2})$ doublet does not form an unobserved excited (bound) state of $^5_\Lambda$He.

Therefore, we have calculated the total cross section, differential cross section, and polarization as a function of energy for the Λ-^{4}He scattering using the potentials of Ref. 2. Because we are interested in the energy range below the inelastic scattering threshold, we have limited the calculation to energies below 10 MeV and thus have included only the $l=0$, 1, and 2 partial waves. In addition to the central potential fitted to the bound state, we have added a derivative spin-orbit potential[4] and explored its consequences for the $l=1$ phase shifts. We find that there is a large low-energy cross section (comparable to that in the n-^{4}He system) and that, as expected, the calculated observables are sensitive to the strength of the spin-orbit interaction. A similar calculation was recently performed by Alexander, Gal, and Gersten[5] using phenomenological Gaussian potentials to represent the central and spin-orbit Λ-^{4}He interaction, in contrast to our use of Λ-n potentials with soft cores. While the qualitative behavior of our results is similar to theirs, the quantitative results are rather different.

In Sec. II, we discuss the Hartree-Fock equations for the bound systems ^{4}He and $^5_\Lambda$He, which